Researching The Dynamic Response Law of High and Steep Subgrade Slopes Using ABAQUS

Jinluan Li [a], Haifeng Bai [b], Suning Li [c]

Dalian Jiaotong University Dalian, China

[a] 1158350848@qq.com, [b] haifeng-bai@163.com, [c] 18742038451@163.com

Abstract. The study aimed to investigate the dynamic response of vehicles traveling on expressways across high and steep subgrade slopes under vehicle loads. This was done by creating a finite element model of high and steep subgrade slopes through ABAQUS software and its secondary program development. Specific engineering examples were used to analyze the dynamic response states and laws of high and steep subgrade slopes under varying vehicle speeds and load conditions. The study's results indicate that: (1) When the vehicle is travelling at 100 km/h, its vibration frequency is close to the natural frequency of the subgrade in the section, leading to strong dynamic responses. (2) As the number of axles increases, the pressure on the contact surface between the wheel and the roadbed rises, and dynamic responses become stronger. The four-axle vehicle shows the most significant dynamic response. (3) The maximum vertical stress fluctuates around an intermediate value over time. (4) The highest maximum vertical displacement value is observed in the penultimate analysis step, with a noticeable peak value. At this point, the vehicle load has the most prominent impact on the roadbed slope.

Keywords: High and steep subgrade; Vehicle moving load; ABAQUS; Secondary development; dynamic response.

1. Introduction

The stability of high fill subgrade slopes is often compromised in mountainous regions due to the intricate and changeable geological conditions. Additionally, external loads, soil properties, and rainfall infiltration are several factors that exacerbate the situation. As a result, engineering safety accidents are more likely to occur in such areas. Moreover, the stability of subgrade slopes becomes even more crucial under the impact of highway vehicle loads. As a result, numerous scholars have conducted extensive research on this topic. Kamaran et al. have devised a program and methodology for stress analysis of rigid pavement on a three-layer foundation. Chen Jian employed ABAQUS finite element software to construct a three-dimensional model of the roadbed. The model was subjected to three distinct vehicle loads, namely static load, moving constant load, and sinusoidal load, to examine the dynamic response of the roadbed under varying vehicle loads. The elastoplastic constitutive relationship of the soil was used as the basis for the analysis. Yu Jianrong adopted a method that combines spatial finite element theory with elastic half space analysis to treat the semi rigid base and rigid pavement as two-layer elastomers resting on an elastic half space foundation. The study analyzed the impact of the connection state between the semi rigid base and rigid surface layers on the load stress. In summary, numerous scholars have investigated the dynamic response analysis methods and patterns of subgrade slopes from various viewpoints and using different numerical analysis techniques.

At present, the majority of research on the dynamic response of subgrade slopes is mainly concentrated on the response characteristics of fixed loads. There is comparatively less research conducted on the response of moving loads with specific amplitudes and migration speeds. To investigate the influence of moving loads and speeds on roadbed slopes and considering the effects of vehicle speed and load variation on highway pavement, the dynamic response characteristics of a high and steep roadbed slope were analyzed using ABAQUS finite element analysis software. The study aimed to determine the most unfavorable situation.

2. Project Overview

The roadbed slope under study is part of the Mengxing Jiangcheng Lvchun Expressway section, which is situated in the Sichuan, Yunnan, and Guizhou plateaus' dry and wet alternating region, and falls within the natural division of the V5 area. The high fill roadbed is primarily located in mountain valleys, characterized by complex terrain and geological conditions. The soil layer along the route is primarily composed of clay, gravelly soil, gravel layer, and weathered rock layer. The expressway pavement comprises asphalt concrete pavement, cement stabilized crushed stone base, and graded crushed stone base from top to bottom. Table I displays the physical and mechanical parameters of every layer of material.

Tab. 1 Material Parameters of Subgrade Slope

Material parameters	Young's modulus E/MPa	Poisson's ratio /μ	Density ρ/(t/m³)	Internal friction angle φ/(°)	Cohesion c /kPa
Asphalt concrete surface course	1200	0.35	2.45	0	0
Cement stabilized crushed stone base	1800	0.25	2.4	0	0
Graded crushed stone base	1600	0.25	2.35	0	0
Subgrade bed surface	190	0.333	1.95	30	80
Bottom surface of subgrade bed	120	0.333	1.9	28	70
Embankment	60	0.35	1.85	25	60
Foundation	40	0.35	1.8	20	50

The expressway comprises of multiple layers, with the surface layer consisting of 18cm thick asphalt concrete. The base layer is made up of 20cm thick cement stabilized macadam, and the lowermost layer is 25cm thick graded macadam. This two-way four-lane expressway is designed for a speed range of 80-120km/h.

3. 3d Subgrade Slope Model And Vehicle Load Simulation

3.1. 3D subgrade slope model

According to the engineering example, a three-dimensional subgrade slope model for a highway was established using ABAQUS finite element software. The model includes a pavement with dimensions of 12.5m horizontally, and the three-dimensional model has a vertical height of 52m. The subgrade slope has a height of 32m, with the first, second, and third grade slope gradients being 1:1.5, 1:1.75, and 1:2, respectively. The slope heights are 8m, 12m, and 12m. The subgrade has a width of 25m, and the carriageway has a width of 2 × 2 × 3.75m, with an intermediate bandwidth of 3.0m (including 2.0m of central separation bandwidth and 0.5m of curb strips on both sides). The hard shoulder has a width of 2 × 3m (including 0.5m of curb width), and the soil shoulder has a width of 2 × 0.75m. The pavement is made of asphalt and, due to the axial symmetry of the subgrade and pavement, a simplified half side model has been adopted. The element type used in the model is an 8-node linear hexahedron element. The mesh division in the model uses a structural division method with hexahedron-shaped elements. To enhance the accuracy of the calculations, the action surface of the wheels on the traffic lane and the lower grid have been refined. Figure 1 illustrates the division of the grid. The directions of the x, y, and z axes of the model are transverse, longitudinal, and depth directions, respectively. They are positive in the transverse direction to the right, positive in the longitudinal direction, and positive in the depth direction.

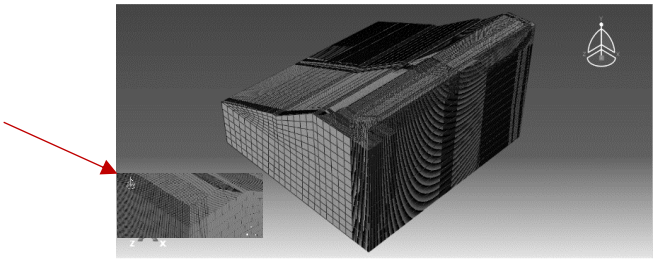

Fig. 1 Grid Division Diagram of Subgrade Slope

3.2. Constitutive model of soil mass

The surface, bottom, embankment, and foundation of the subgrade bed are modeled using the Mohr Coulomb shear failure constitutive model, based on the subgrade and pavement structure of the project. The shear yield surface function in the Mohr Coulomb model is:

$$F = R_{mc}q - p\tan\varphi - c = 0 \quad (1)$$

The friction angle of the material, which is the inclination angle of the Mohr Coulomb yield surface on the $q-p$ stress surface, is represented by φ and has a range of $0° \le \varphi \le 90°$. The cohesion of the material is denoted by c. The polar deviation angle, θ, is defined as $\cos(3\theta) = r^3/q^3$, where r is the third deviator stress invariant J_3.

3.3. Boundary Conditions

In order to allow the subgrade soil mass to slide downward along the boundary, appropriate boundary conditions have been assigned to all five surfaces, with the exception of the surface of the subgrade slope. Specifically, the left and right sides of the subgrade have been constrained in the z-direction for displacement, while the front and rear sides have been constrained in the x-direction for displacement. The bottom surface of the subgrade has been fixed in place. When conducting dynamic analysis of subgrade slopes, the dynamic explicit analysis method is employed.

3.4. Vehicle moving load

To incorporate moving vehicle loads in ABAQUS, secondary development of subroutines is necessary. The first step in incorporating a vehicle moving load in ABAQUS is to simplify the load. This involves simplifying the contact surface between the wheel and the ground to a rectangular shape measuring 0.64m x 0.44m. Next, the vehicle axle is treated as a static load that is uniformly distributed across the contact surface. Using this approach, the force acting on each wheel contact surface can be determined. The subroutine for incorporating the vehicle moving load in ABAQUS can be written using VDLOAD. This involves defining the vehicle speed, determining the range of wheel action on the subgrade surface through x-axis and z-axis coordinates, defining the distributed pressure on the contact surface, and defining it as the road moving load.

4. Dynamic Response Analysis Of High And Steep Subguade Slope Under Vehicle Load

4.1. Dynamic response analysis of subgrade under different vehicle speeds

In this study, we have chosen a two-axle truck as the subject of research. Our aim is to examine the dynamic response patterns of the highway subgrade slope at varying speeds of 80 km/h, 100 km/h, and 120 km/h. The two-axle freight car under consideration has four wheels, with a body length of 9.6m. The two-axle wheelbase is 7.16m, the wheel track width is 1.9m, and the width of each wheel is 29.5cm. The calculated wheel pressure for this freight car is 78.44kPa. Dynamic response results of the subgrade slope surface under three vehicle speeds were obtained using ABAQUS finite element software.

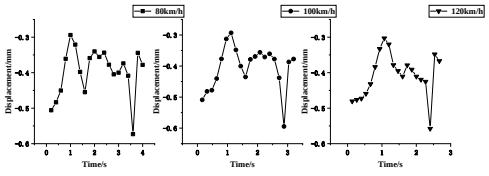

Fig. 2 Maximum Displacement Time History Curves at 80km/h, 100km/h, and 120km/h

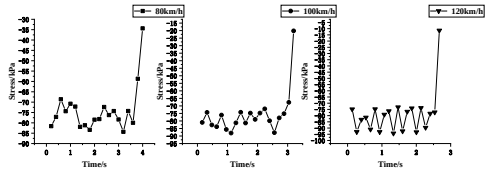

Fig. 3 Maximum Stress Time History Curves at 80km/h, 100km/h, and 120km/h

4.2. Maximum displacement time history curve at different vehicle speeds

Figure 2 illustrates the variation of maximum vertical displacement with time for two-axle freight cars operating at different speeds. The analysis focuses on the maximum displacement time history variation curve of the subgrade at driving speeds of 80 km/h, 100 km/h, and 120 km/h. The analysis indicates that the maximum vertical displacement time history follows a similar trend at all three driving speeds. It is observed that the maximum vertical displacement decreases gradually before 1s, reaching its minimum value at this point. This is due to the reverse bending moment generated by the subgrade, which gradually increases and causes a decrease in the vertical displacement caused by the vehicle loads. From 1s to 1.5s, the reverse bending moment decreases, and the vertical displacement gradually increases. The maximum vertical displacement occurs in the penultimate analysis step, and there is a noticeable peak value. This indicates that the vehicle load has the most significant impact on the roadbed slope at this point. Moreover, the maximum displacement peak value remains almost the same at different speeds, suggesting that the driving speed has little effect on the maximum displacement.

4.3. Maximum stress time history curve at different vehicle speeds

Figure 3 shows the maximum stress time history variation curve of the subgrade at driving speeds of 80 km/h, 100 km/h, and 120 km/h. Through comparative analysis, it is observed that the time history variation trend of the maximum vertical stress is approximately the same at all three driving speeds. Additionally, it can be observed that the maximum vertical stress time-history curve follows a zigzag pattern at all three vehicle speeds, fluctuating around an intermediate value. Furthermore, as the driving speed increases, the intermediate value of the maximum vertical stress also increases. However, within the range of driving speeds from 100 km/h to 120 km/h, the intermediate value does not change significantly. This suggests that the maximum vertical stress increases as the vehicle speed increases. This can be attributed to the increase in impact force on the subgrade surface as the vehicle speed increases. As a result, the greater force on the subgrade due to the increased impact force results in an increase in the maximum vertical stress. It is also noted that the three curves exhibit a rapid approach to zero in the final analysis step. This phenomenon can be explained by the successive departure of vehicle axles from the active subgrade surface, leading to a rapid decrease in the maximum vertical stress, which eventually approaches zero.

4.4. Dynamic response analysis of subgrade under different axle numbers

In this study, we investigate the dynamic response of freight cars to highway subgrade slopes at a speed of 100 km/h, considering the number of axles as two, three, and four. The characteristics of each type of freight car used in the analysis are as follows:(1) Two-axle freight car: Four wheels, body length of 9.6m, two-axle wheelbase of 7.16m.(2) Three-axle freight car: Six wheels, body length of 9.6m, front and middle axle wheelbase of 5.7m, middle and rear axle wheelbase of 1.35m.(3) Four-axle freight car: Four wheels, body length of 9.6m, axle wheelbases from front to rear of 2.05m, 4.4m,

and 1.35m.(4) Wheel track width: 1.9m.(5) Wheel width: 29.5cm. According to our calculations, the wheel pressure for each type of freight car is as follows:(1) Two-axle freight car: 78.44 kPa. (2) Three-axle freight car: 87.16 kPa. (3) Four-axle freight car: 87.16 kPa. The dynamic response of the subgrade slope surface under the three different axle numbers was analyzed using ABAQUS finite element software.

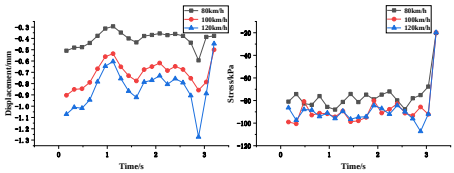

Fig. 4 Maximum displacement and stress time history curve of two axle, three axle, and four axle freight carsFigures and Tables

4.5. Maximum displacement time history curve under different axle numbers

In this analysis, we focused on studying the variation of vertical maximum displacement over time for a freight car traveling at a speed of 100 km/h, using different numbers of axles as the research object. The total analysis step was also taken into consideration. The variation curve of the maximum displacement time history for the subgrade under the influence of trucks with two axles, three axles, and four axles is depicted in Figure 4. According to the analysis, the trend of the maximum vertical displacement time history remains relatively consistent. Simultaneously, it was observed that the highest vertical displacement for all three axle numbers occurred during the second to last analysis step, showing a distinct peak value. This suggests that the vehicle load has the most significant impact on the slope of the roadbed at this particular moment. It can be also observed that there is a positive correlation between the number of axles and the overall maximum vertical displacement. In other words, as the number of axles increases, so does the maximum vertical displacement. The reason behind this correlation is that an increase in the number of axles leads to an increase in the weight of the vehicle body. As a result, the pressure exerted on the contact surface between the wheels and the roadbed also increases, leading to a higher dynamic response to roadbed displacement.

4.6. Maximum stress time history curve under different axle numbers

Figure 4 illustrates the time history curve of the maximum stress experienced by the subgrade under the driving of trucks with two, three, and four axles. According to the analysis, the time history of the maximum vertical stress exhibits a similar variation trend. Additionally, it is worth noting that the time-history curve of the maximum vertical stress for all three axle configurations exhibits a zigzag pattern, with the stress level fluctuating around an intermediate value. As the number of axles increases, the intermediate value also tends to increase. This phenomenon can be attributed to the fact that as the number of axles increases, the weight of the vehicle body also increases. This results in a higher pressure being exerted on the contact surface between the wheels and the roadbed, leading to an increase in the dynamic stress response of the roadbed. As a result, the maximum vertical stress experienced by the subgrade also increases. Furthermore, in the final analysis step, it is observed that the changes in the three time-history curves rapidly approach zero. This is because the axles of the vehicle have successively left the surface of the roadbed, leading to a rapid decrease in the maximum vertical stress. Ultimately, the stress level tends towards zero as all axles move away from the roadbed surface.

5. Conclusion

(1) The analysis reveals that when the vehicle travels at a speed of 100 km/h, the displacement and stress dynamic response of the roadbed slope are more pronounced in comparison to when the vehicle travels at 80 km/h or 120 km/h. This observation suggests that the vibration frequency generated by

the vehicle traveling at 100 km/h is closer to the natural frequency of the roadbed in this section, resulting in a stronger dynamic response.

(2) The analysis also indicates that the dynamic response of a four-axle vehicle to the displacement and stress of the roadbed slope is more pronounced than that of a two-axle or three-axle vehicle. This observation supports the idea that as the number of axles increases, the pressure on the contact surface between the wheels and the roadbed also increases, resulting in a stronger dynamic response. Therefore, when a vehicle with four axles travels at 100 km/h, it creates the most unfavorable situation for the high and steep subgrade slope in this project. At this point, the dynamic displacement and dynamic stress response of the high and steep subgrade slope are the most significant.

(3) The time-history curve of the maximum vertical stress at three different vehicle speeds exhibits a zigzag pattern, with the stress level fluctuating around an intermediate value. Furthermore, this intermediate value tends to increase as the driving speed increases. Within the range of 100 km/h to 120 km/h, the intermediate value does not change significantly.

(4) The analysis reveals that the maximum value of the maximum vertical displacement occurs in the penultimate analysis step, and a relatively significant peak value is observed. This observation suggests that the vehicle load has the most substantial impact on the subgrade slope at this point in time.

Acknowledgments

I would like to acknowledge Professor, Haifeng Bai, for providing me with the engineering background information.

My research partner, Suning li, was instrumental in defining the path of my research. For this, I a m extremely grateful.

With many thanks to my supervisor, Haifeng Bai, for his guidance during this research.

References

[1] Fei, K., Zhang, J.,Application of ABAQUS in geotechnical engineering. Beijing, China: China Waterpower Press, 2010.

[2] Deng, X, Subgrade and pavement engineering. 3rd ed. Beijing, China: People's Communications Press, 2008.

[3] Sha, A, Subgrade and pavement engineering. Beijing, China:Higher Education Press, 2011.

[4] Chen, Y, Numerical simulation study on the impact of traffic load on low embankment highway subgrade. [Dissertation]. Hohai University, 2006.

[5] Fan, Y. Analysis and research on subgrade response under traffic load. [Dissertation]. Central South University, 2008.

[6] Li, B., Gao, Y., Wei, D., et al., Study on the depth of influence and influencing factors of vehicle load. Rock and Soil Mechanics, 2005(S1): 4.

[7] Chen, J. and Su, Y.,Numerical simulation study on the dynamic characteristics of highway subgrade under traffic load. Highway Traffic Science and Technology, 2011, 028(005): 44-48.

[8] Cao, Y., Liang, N., Yu, Q., et al., Calculation method for dynamic load of vehicles caused by road roughness. Journal of Traffic and Transportation Engineering, 2008, 8(2): 5.